

Phase Behaviour Study and Spectroscopic Characterization of Quantum Dots- Polymer Self-Assembled Aggregates

M.Sc. Thesis

By

Punam Pawe



DISCIPLINE OF CHEMISTRY
INDIAN INSTITUTE OF TECHNOLOGY INDORE

June, 2019

Phase Behaviour Study and Spectroscopic Characterization of Quantum Dots- Polymer Self-Assembled Aggregates

A THESIS

*Submitted in partial fulfilment of the
Requirements for the award of the degree
Of
Master of Science*

By
Punam Pawe



**DISCIPLINE OF CHEMISTRY
INDIAN INSTITUTE OF TECHNOLOGY INDORE
June, 2019**



INDIAN INSTITUTE OF TECHNOLOGY INDORE

CANDIDATE'S DECLARATION

I hereby certify that the work which is being presented in the thesis entitled **Phase Behaviour Study and Spectroscopic Characterization of Quantum Dots-Polymer Self-Assembled Aggregates** in the partial fulfilment of the requirements for the award of the degree of **MASTER OF SCIENCE** and submitted in the **DISCIPLINE OF CHEMISTRY, Indian Institute of Technology Indore**, is an authentic record of my own work carried out during the time period from July, 2017 to July, 2019, under the supervision of Dr. Tushar Kanti Mukherjee, Associate Professor of IIT Indore.

The matter presented in this thesis has not been submitted by me for the award of any other degree of this or any other institute.

Signature of the student with date
Punam Pawe

This is to certify that the above statement made by the candidate is correct to the best of my/our knowledge.

Signature of Thesis Supervisor
Date:

Punam Pawe has successfully given his/her M.Sc. Oral Examination held on **1-07-2019**

Signature(s) of Supervisor(s) of MSc thesis
Date:

Convener, DPGC
Date:

Signature of PSPC Member #1
Date:

Signature of PSPC Member #2
Date:

Signature of PSPC Member #3
Date:

ACKNOWLEDGEMENTS

With great pleasure I would like to express my deep sense of gratitude to my supervisor Dr. Tushar Kanti Mukherjee for giving me this opportunity to pursue research and believing in me. His constant guidance and support to complete this M.Sc. project. Further I would like to thank my PSPC members Dr. Suman Mukhopadhyay, Dr. Satya S. Bulusu and Dr. Apurba K. Das for their support.

I would like to express my gratitude to Prof. Pradeep Mathur, Director IIT Indore, for his continuous encouragement and support in every aspect.

I am grateful to Dr. Amarendra K. Singh (Head, discipline of Chemistry, IIT Indore) for his suggestion. I am also grateful Prof. Rajneesh Mishra, Dr. Sanjay K. Singh, Dr. Tridip K. Sarma, Dr. Biswarup Pathak, Dr. Chelvam Venkatesh, Dr. Sampak Samantha and Dr. Anjan Chakraborty, for their guidance and help during various activities.

I extend my heartiest thanks to my PhD mentor Miss Jamuna K. Vaishnava, for her constant selfless guidance and also Miss Bhawna for her valuable support.

I would like to thank the technical staff from SIC, IIT Indore, Mr. Kinny Pandey, Mr. Ghanashyam Bhavsar, Dr. Ravinder and Mr. Manish Kushwaha for their patience and timely technical support without which it was impossible to continue with my project work.

I personally want to extend my thanks to my fellow batch mates and friends Barsha Deori, Vanitha Naina Reddy, Puja Singhvi, Mahima Rajput and Sandhya Jaiswal who were always there to encourage me during my M.Sc. days.

I would like to thank IIT Indore for infrastructure and all other help and lastly, I would express my deepest appreciation for my beloved my parents, throughout these years that I have studied.

PUNAM PAWE
CHEMISTRY

Abstract

Here we present a simple and flexible method for the synthesis MSA-capped CdTe QDs by coacervation with oppositely charged polyelectrolyte, poly(diallyldimethylammonium chloride) PDADMAC. A continuous series of different phases, from initially clear (C_1) to turbid (T_1) then precipitate (P), turbid (T_2) and clear (C_2) has been observed for QD solution upon increasing the concentration of polyelectrolyte solution. However, no such variation is observed in case of neutral PVP (Polyvinylpyrrolidone), indicating specific electrostatic interaction behind the observed phase behaviours. The morphologies and photoluminescence properties of the coacervates in the T_1 and T_2 regions were explored using field emission scanning electron microscopy (FESEM). These luminescent coacervates are quite stable in neutral and basic pH (pH- 6.7- 10), whilst, very much unstable in acidic pH (pH- 3-5). Ionic strength study of T_1 and T_2 region is carried out with NaCl. We have further demonstrated the efficient encapsulation of dyes and proteins – FITC, Rhodamine 6G, Nile blue, HSA and BSA into the colloidal droplets without any structural disruption. A simple system for encapsulation like the one presented here might be useful for a range of different application such as drug delivery, bioimaging and sensing.

Table of Content

LIST OF FIGURES	xi-xii
LIST OF TABLE	xiii
NOMENCLATURE	xv
ACRONYMS	xvii
Chapter 1: Introduction	1-5
1.1. Quantum Dots	1-2
1.1.1. Quantum Confinement	2-3
1.2. Polyelectrolyte	3-5
Chapter 2: Experimental Section	7-9
2.1. Materials	7
2.2. Synthesis of MSA-capped CdTe QDs	7-8
2.3. Instrumentation	8
2.4. Sample Preparation QD-PDADMAC	8-9
Chapter 3: Result and Discussion	11-19
3.1. Characterization of MSA-capped CdTe QDs	11-12
3.2. Phase behavior of the binary mixture of CdTe QD and oppositely charged polyelectrolyte solution of PDADMAC.	12-13
3.3. PL behavior of GQD-PDADMAC binary mixture in the C1 and. C2 region	13-15
3.4. Formation of Coacervation and colloidal droplets	15-16
3.5. The effect of variation of pH and ionic strength on the colloidal droplets formed in T1 and T2 region	16-17
3.6. Dye and protein loading	17-19
Chapter 4: Conclusion	20
REFERENCES	21-23

List of Figures

Figure 1.1	Schematic comparison of electronic states of bulk semiconductor vs. quantum dots	2
Figure 1.2	Structural representation of Poly-(diallyldimethylammonium chloride) (PDADMAC); Poly(sodium-4-styrenesulfonate) (PSP); Poly(acrylic acid) (PAA); Polyethylenimine (PEI).	4
Figure 1.3	Polymerisation of PolyDADMAC (with respect to pyrrolidine structure)	5
Figure 2.1	The synthesis procedure of MSA-capped CdTe QDs	7
Figure 3.1	(A) Absorption and (B) Photoluminescence (PL) spectra of green QDs. (C) FTIR spectra of as prepared MSA capped CdTe Quantum dot. (D) AFM image of green QD.	10
Figure 3.2	(A) Phase behaviour of the binary mixtures as a function of PDADMAC concentration. (B) Turbidity Vs [PDADMAC] plot keeping absorbance at 650nm with molar concentration of PDADMAC in the binary mixture.	11
Figure 3.3	Variation in the (A) absorption spectra, (B) PL spectra ($\lambda_{ex} = 450$ nm), for the initial concentration of PDADMAC and. (D) FESEM image of QD-PDADMAC binary mixture in C1 region.	12
Figure 3.4	(A) Absorption spectra of QD-PVP binary mixture from 10mM-160mM. (B) Intensity ratio Vs [PVP] (mM)..	13

- Figure 3.5** FESEM images of the binary mixtures in the (A) T1, and (B) T2 regions of the phase profile. **14**
- Figure 3.6** (A) Photograph of the binary mixture of pH-3 and pH-10 upon addition of (i) HCl and NaOH. (ii) Salt solution at different concentration ionic (B) variation in the turbidity of the binary mixture with respect to pH in the T1 and T2 regions. (B) variation in the turbidity of the binary mixture with respect to different concentration of NaCl in the T1 and T2 regions. **15**
- Figure 3.7** Absorption spectra of (a) FITC, (b) Rh6g, (c) Nile blue, (d) HSA and (e) BSA with T2 (130 μ M). The black curve represents the dyes and protein in aqueous solution. **17**

List of Table

Table 1.	Estimated partition coefficients (K) of dyes and proteins inside coacervate droplets (T2 region).	19
-----------------	---	-----------

ACRONYMS

QD	Quantum Dot
CdTe	Cadmium Telluride
CdSe	Cadmium Selenide
MSA	Mercaptosuccinic acid
PDADMAC	Poly(diallyldimethylammonium chloride)
PVP	Polyvinylpyrrolidone
PEI	Polyethylenimine
PL	Photoluminescence
FTIR	Fourier Transform Infrared
FESEM	Field Emission Scanning Electron Microscopy
λ_{ex}	Excited wavelength
FITC	Fluorescein isothiocyanate
Rh6G	Rhodamine 6G
HSA	Human serum albumin
BSA	Bovine serum albumin

NOMENCLATURE

M	Molar
mM	Milimolar
μ M	micromolar
nm	Nanometer
ns	nanosecond
rpm	Revolution per minute
mL	milliliter
h	hour
$^{\circ}$ C	Degree centigrade
mg	milligrams

Chapter 1

Introduction

In this modern society the technological advancements are proceeding with an outstanding pace which is unequalled by any previous historical era. However, continuation of such advances places extensive amount of pressure on scientists and demands new discovery and development of new and improved technologies, materials, medicines, devices, etc. The fields of nanoscience and nanotechnology are focused mainly on materials in the nanoscale, i.e., in the dimension less than 100 nm. These small sizes are expected to increase the ratio of surface area to volume of the nanostructure materials, which in turn increases the interfacial surface area. [1] Two primary techniques for preparing nanoscale materials are bottom-up and top-down. The bottom-up method uses small building blocks as starting materials and muster them into larger structures. Some examples of bottom-up method includes chemical synthesis, [2, 3] laser-induced assembly, [4,5] self-assembly, [6] colloidal aggregation, [7] In the top-down method bigger objects are modified to give smaller In the top-down approach large objects are modified to give smaller features by destructing a section of the actual structure.

1.1. Quantum Dots

Focussing on the semiconductor materials within nanoscale dimension in recent researches have led to the production of an interesting class of novel materials which possess characteristic features of both bulk and molecular semiconductors. These are nanocrystalline semiconductor materials that show properties such as quantum confinement, and are thus referred to as 'Quantum Dots'. Quantum dots are gaining booming scientific interest due to their unique optical and

electrical properties and advancement in synthetic approaches. These advances have resulted in many applications in case of biology, [8-11] biosensing, [12-14] and optoelectronics. [15] Quantum dots are generally semiconductor nanocrystals or nanoparticles in which excitons (electron and electron-hole pair) are confined in all three spatial dimensions.

1.1.1. Quantum confinement effect

Quantum confinement effect is generally observed when the radii of the nanocrystal is smaller than the average distance between the electron and the electron hole, commonly known as the bulk excitonic Bohr radius. A useful model to understand the electronic states of these spherical nanocrystals, is the particle in a box. The electron and the hole are constricted into a relatively small space by a potential that is infinite at the nanocrystal surface. As a result, semiconductors of nanoscopic dimensions have larger band gaps than bulk material, and have discrete energy levels (Figure 1.2). [16-27] such features are characteristic of the molecular regime rather than the bulk. The intermediate nature of quantum dots, with characteristics of both bulk and molecular materials, explains the enthusiasm that drives the exploration of quantum dot based applications.

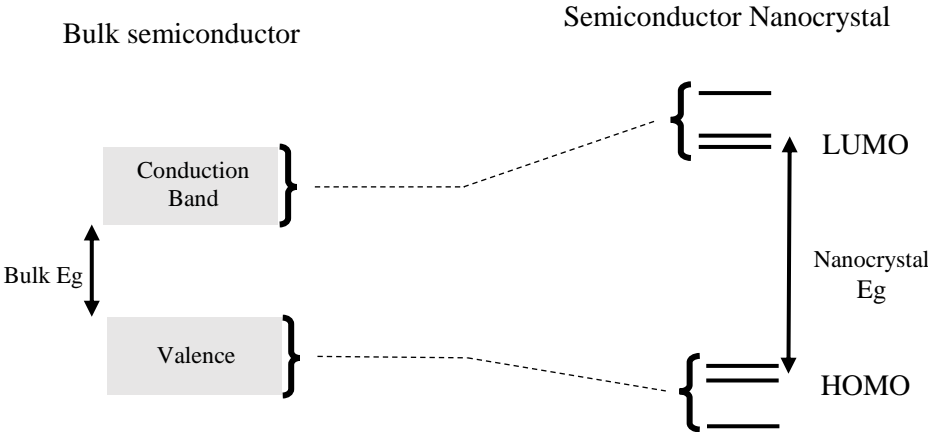


Figure 1.2. Schematic comparison of electronic states of bulk semiconductor vs. quantum dots

1.2. Polyelectrolytes

Polymer materials are widely used in all aspects of our lives. Rapid development of polymer research contributes to amount of meaningful applications, such as in the region of batteries [28-29] and hydrogels [30, 31, 32]. These are simply water soluble polymer which carries ionic charge along the polymer chain and are commonly used in the research of complex coacervation. They are defined as linear macromolecule chains bearing a large number of chargeable groups and usually dissolved in polar solvent, generally water [33]. In positively (or negatively) charged polyelectrolyte solution, a single species polymer with random polydispersity and one species of counter-ions which are small ions with oppositely charged sign to that of macromolecular charge are present [33]. The charge of counter-ion and macromolecule must be in equivalent order to attain the condition of electroneutrality [34]. Depending upon the degree of charging, polyelectrolyte can be divided into two types, including strong polyelectrolyte which completely dissociates in solution and weak polyelectrolyte which is partially charged in solution. The structures of some broadly used strong polyelectrolytes and weak polyelectrolytes are illustrated in the Figure 1.2. Polyelectrolyte has many applications, mostly related to providing surface charge to neutral particles leading to well-dispersion in aqueous solution. Due to specific properties, polyelectrolytes are often used as emulsifiers, conditioners, Thickening agent, dispersant, suspension stabilizer, adhesive, soil conditioner, paper strengthening agent, fabric antistatic agent and so on.

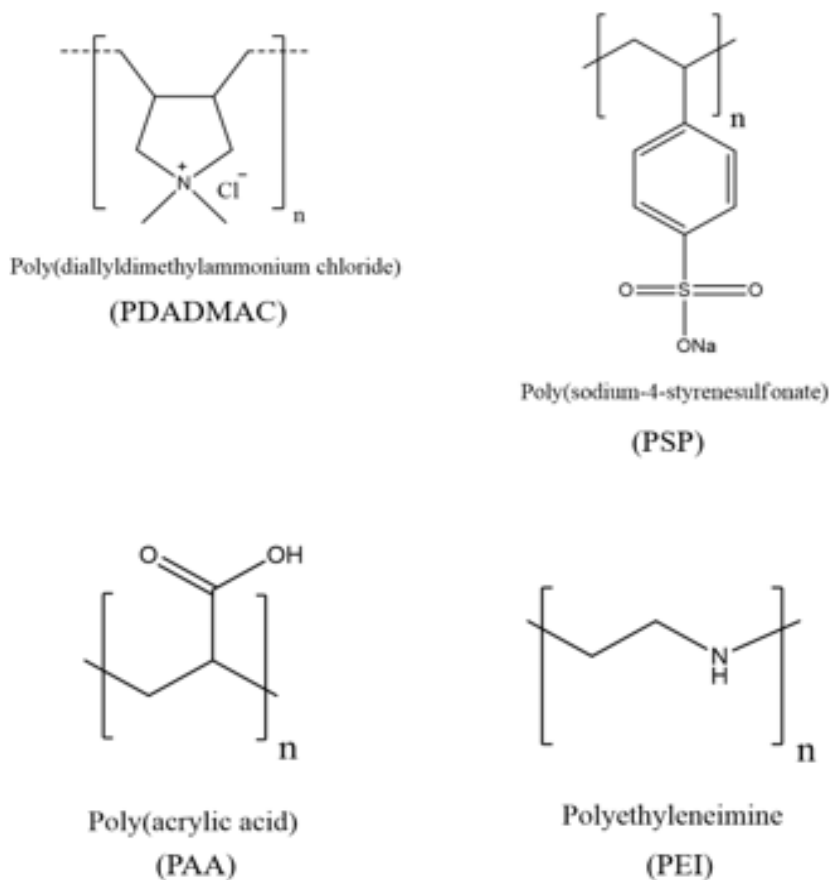


Figure 1.2: Structural representation of Poly(diallyldimethylammonium chloride) (PDADMAC); Poly(sodium-4-styrenesulfonate) (PSP); Poly(acrylic acid) (PAA); Polyethylenimine (PEI).

1.2.1. Poly(diallyldimethylammonium chloride) (PDADMAC)

Poly(diallyldimethylammonium chloride) also known as polyDADMAC or polyDDA is a homopolymer of diallyldimethylammonium chloride (DADMAC). It is a high charge density cationic polyelectrolyte. The monomer DADMAC is obtained by reacting two equivalents of allyl chloride with that of dimethylamine. PDADMAC is synthesized by radical polymerization of DADMAC with an organic peroxide used as catalyst. When polymerizing DADMAC two polymeric structures are possible: N-

substituted piperidine structure or N-substituted pyrrolidine structure, out of which pyrrolidine structure is favoured. [21]

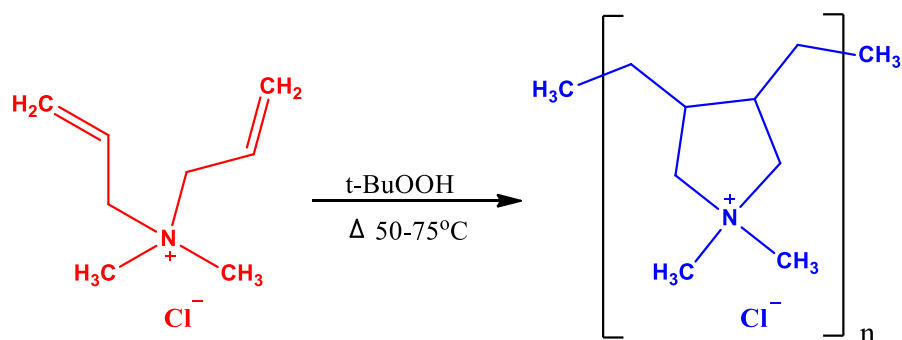


Figure 1.3: Polymerisation of PolyDADMAC (with respect to pyrrolidine structure)

As we know that coacervation, also known as phase separation, is a process of separation of a liquid phase coating material from a polymeric solution and wrapping of that phase as a uniform layer around suspended core particles, we have applied this technique to fabricate a new class luminescent hybrid coacervate droplets from CdTe quantum dots (QDs) and poly(diallyldimethylammonium chloride) (PDADMAC) aqueous mixture. The stability of these hybrid colloidal droplets has been explored by a wide range of factors such as composition, pH, and ionic strength. The present study can be easily extended to create a variety of hybrid droplets with various inorganic organic counterparts having unique optoelectronic properties, which will further expand their applicability in nanocatalysis, bioimaging and biosensing.

Chapter 2

Experimental Section

2.1 Materials used

For the synthesis CdTe Quantum Dots, Cadmium chloride Sodium tellurite (Na_2TeO_3), Tri-sodium citrate ($\text{Na}_3\text{C}_6\text{H}_5\text{O}_7 \cdot 2\text{H}_2\text{O}$), Mercaptosuccinic acid (MSA) ($\text{C}_4\text{H}_6\text{O}_4\text{S}$) Sigma-Aldrich, St. Louis, MO, USA and Sodium Borohydride (NaBH_4) were purchased from SRL. Hydrochloric acid (HCl), Sodium hydroxide (NaOH) and Sodium chloride (NaCl). Rhodamine 6G, Nile blue, fluorescein isothiocyanate (FITC), Human Serum Albumin (HSA), Bovine Serum Albumin (BSA), Polyvinylpyrrolidone (PVP, MW = 40 000), hellmanex III, Pur-A- Lyzer dialysis kit (molecular weight cut-off 3.5 kDa), purchased from Sigma-Aldrich. Mili-Q water was obtained from a Millipore water purifier system (Mili-Q integral).

2.2. Synthesis of MSA-capped CdTe QDs

The MSA-capped CdTe QDs are synthesized by a previously reported method. [35-36]. The synthesis is carried out by diluting CdCl_2 (22.4 mg, in 4mL) into a one-necked round bottom flask. With constant stirring and maintain room temperature, tri-sodium citrate (100mg), sodium tellurite (2.20 mg, 1mL), MSA (50mg) and NaBH_4 (100mg) were added. When the colour of the solution turns greenish the RB is attached to a condenser and refluxed for approx. 20mins keeping the temperature constant. The resulting QDs were then purified by dialysis for 24 h. The final product was kept in the dark at 4°C and for further use. The size and concentration of CdTe QDs were calculated by the equation proposed by Peng. [40]

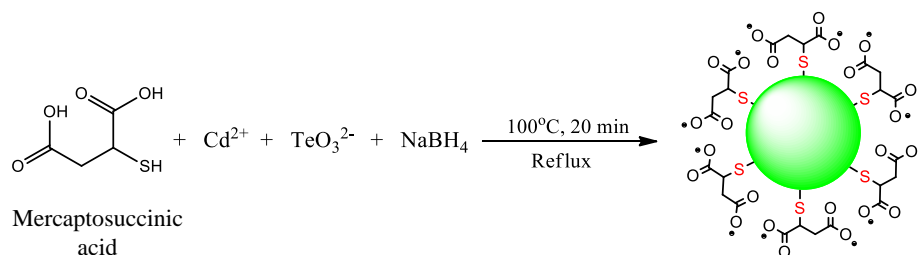


Figure 2.1: The synthesis procedure of MSA-capped CdTe QDs

2.3. Instrumentation

- The spectra for UV-Vis were carried out in a quartz cuvette ($10 \times 10 \text{ mm}^2$) by using a Varian UV-Visible spectrophotometer (Carry 100 Bio).
- Photoluminescence (PL) spectra were carried out using a Fluoromax-4 Spectrofluorometer (HORIBA Jobin Yvon, model FM-100) with excitation and emission slit width at 5nm. All the measurements were performed at room temperature.
- Fourier Transform Infrared (FTIR) measurements were recorded in a Bruker spectrometer (Tensor-27) on a thin film of KBr made into small transparent pellet.
- Atomic Force Microscopy (AFM), images were taken on a clean glass coverslip using AIST-NT microscope (model SmartSPM-1000). The sample was drop-casted onto each slide.

2.4. Preparation of QD-Poly(diallyldimethyl-ammonium chloride) solution and Quantum yield estimation.

Different binary mixtures of QDs and PDADMAC were prepared in Milli-Q, keeping the overall concentration of QDs fixed at $0.33 \mu\text{M}$, while the concentration of PDADMAC was varied from 1.3 - $5000 \mu\text{M}$. All the binary mixtures were incubated for 12 h before any further measurements. Similarly, binary mixtures of QDs-PVP were prepared

using different concentrations of PVP into 0.33 μM aqueous solutions of QDs. The pH of the solution was balanced by adding proper amount of stock solution of HCl and NaOH into the binary mixture. The ionic strength was varied by adding proper amount of stock solution of NaCl (1M) into the binary mixture. The luminescence quantum yield (QY) of CdTe QDs was estimated relative to Rhodamine 6G ($\phi_f = 0.95$) in water by using the following equation:

$$\phi_{\text{QD}} = \phi_{\text{ST}} \left(\frac{I_{\text{QD}}}{I_{\text{ST}}} \right) \left(\frac{\eta_{\text{QD}}^2}{\eta_{\text{ST}}^2} \right) \left(\frac{A_{\text{ST}}}{A_{\text{QD}}} \right) \quad (1)$$

where ϕ is Quantum Yield, I is the integrated fluorescence intensity, η is the refractive index of the solvent, and A is the optical density. The subscript 'ST' stands for standard and 'QD' stands for the CdTe QDs sample. The estimated luminescence Quantum yield of QD is 0.20.

Chapter 3

Result and Discussion

3.1 Characterization of MSA-capped CdTe QDs

The as synthesized CdTe QDs are characterized using UV-vis, Fluorimeter, SEM and FTIR spectroscopic techniques. Figure 3.1 (A) and (B) shows the absorption and emission spectra of MSA-capped CdTe Quantum Dot

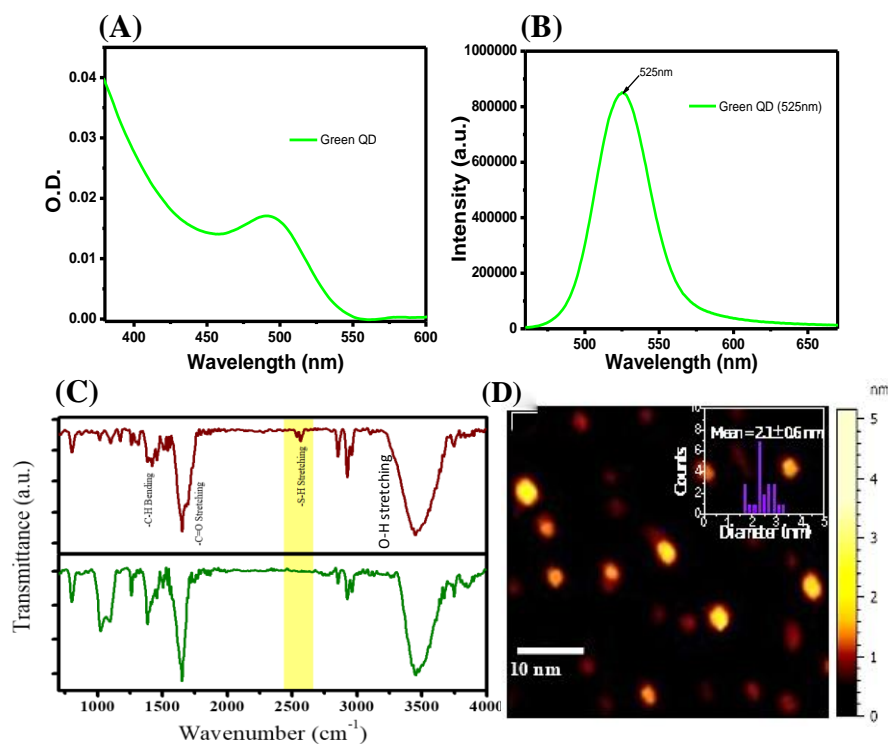


Figure 3.1: (A) Absorption and (B) Photoluminescence (PL) spectra of green QDs. (C) FTIR spectra of as prepared MSA capped CdTe Quantum dot. (D) AFM image of CdTe Quantum Dots.

The broad absorption spectrum in Figure 3.1 (A) is characterized by exciton band maximum at 490 nm. The mean size of the QDs was calculated from Peng equation [40] and was found to be 2 nm. The emission spectrum in Figure 3.1 (B) shows a PL band maximum at 525nm. To confirm that MSA ligand has attached covalently to the surface of QDs, FTIR spectroscopy was performed. The characteristic peak observed at 2500 cm^{-1} is that of S-H_{stretch} vibration of the free MSA ligand. This S-H_{stretch} peak (bottom spectra) disappears after MSA gets covalently attached to the surface of the QD through its free thiol. The broad absorption peak observed at 3432 cm^{-1} is due to O-H_{stretch} vibration, the absorption band at $1550\text{-}1600\text{ cm}^{-1}$ due to C=O vibration was observed in case of both the free MSA ligand and after it got attached to the QDs surface.

3.2. Phase behaviour of the binary mixture of CdTe QD and oppositely charged polyelectrolyte solution of PDADMAC.

A continuous phase sequence from clear C1 to turbid T1, precipitate P, turbid T2 and to clear C2 is observed when QD is mixed with oppositely charged PDADMAC polymer in the range from 1.3-5000 μM . Figure 3.2 (A) is a diagrammatical representation of all the concentration of polymer falling under the three phases Clear, Turbid and Precipitate. The initial few concentrations are clear and isotropic in nature, later it turns turbid then precipitate, again turns turbid and finally clear as the concentration of polymer is increased gradually. However the concentration of QD is kept constant at $0.33\text{ }\mu\text{M}$. Figure 3.2 (B), shows the plot of turbidity against different molar concentration of PDADMAC. The two highest points in the graph represents the concentration at which the solution becomes turbid.

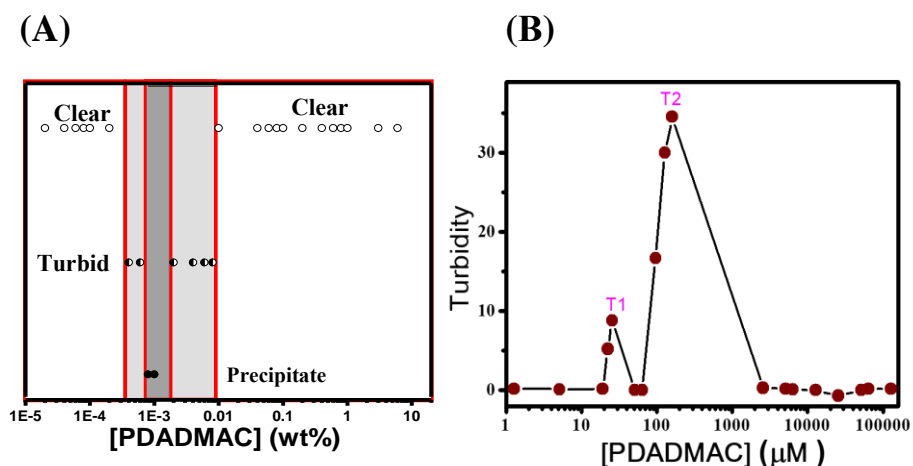


Figure 3.2: (A) Phase behaviour of the binary mixtures as a function of PDADMAC concentration. (B) Turbidity Vs [PDADMAC] plot with molar concentration of PDADMAC in the binary mixture.

3.3. PL behaviour of GQD-PDADMAC binary mixture in the C1 and C2 region.

Aqueous solutions of QDs and PDADMAC were mixed in to prepare different binary mixtures. The overall concentration of QD was kept constant at 0.33 μM , while that of PDADMAC was varied in the range of 1.3-5000 μM . All the binary mixtures were incubated for 12 h before further measurements. The binary mixtures at the initial PDADMAC concentrations (1.3-19.2 μM) are all isotropic. The absorption peak of QD remains almost same, while the absorption band gets broaden.

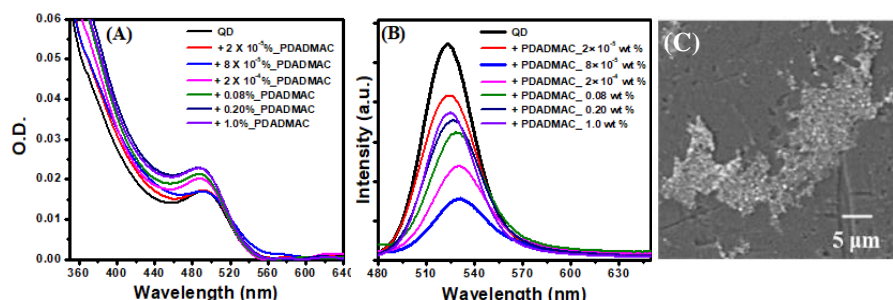


Figure 3.3: Variation in the (A) absorption spectra, (B) PL spectra ($\lambda_{\text{ex}} = 450 \text{ nm}$), for the initial concentration of PDADMAC and. (C) FESEM image of QD-PDADMAC binary mixture in C1 region.

Notable changes have been observed in the PL spectrum of QD-PDADMAC binary mixture (Figure 3.3 b). The peak position of QD in the PL spectra shifts from 523 to 531 nm upon addition of $5.2 \mu\text{M}$ (blue line) of PDADMAC with a red shift of 8 nm. The intensity of QD also decreases upon addition of $5.2 \mu\text{M}$ of PDADMAC. Similar red-shift with decrease in PL intensity has been observed in the presence of different concentrations of PDADMAC in the range of 1.3-19.2 μM .

The FESEM image of the binary mixture at $5.2 \mu\text{M}$ of PDADMAC (C1) reveals the formation of QD-PDADMAC nanocomposites (Figure 3.3.D). The red shift observed at the initial C1 is due to formation of some kind of aggregates. The significant quenching of the PL intensity is due to exciton-exciton coupling between two different QDs at close proximity in the nanocomposite formed. To clearly have an insight of the nature of interaction between QD-PDADMAC, controlled experiment of QD with neutral Polyvinylpyrrolidone (PVP) is carried out, where it is seen that the intensity ratio is almost negligible at different PVP concentration.

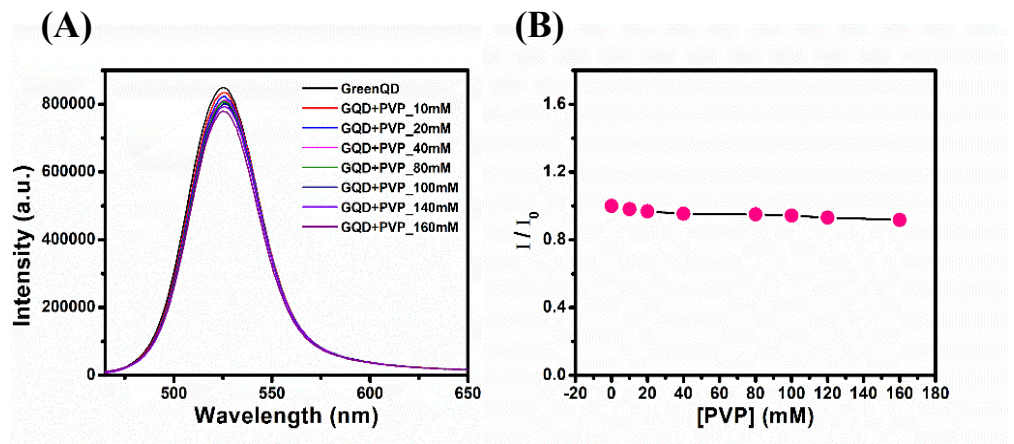


Figure 3.4: (A) Absorption spectra of QD-PVP binary mixture (B) Intensity ratio Vs PVP (mM).

3.4. Formation of Coacervation and colloidal droplets

In the T1 and T2 regions of the binary mixture the appearance of turbidity indicates self-assembled structure. (Figure 3.5.)

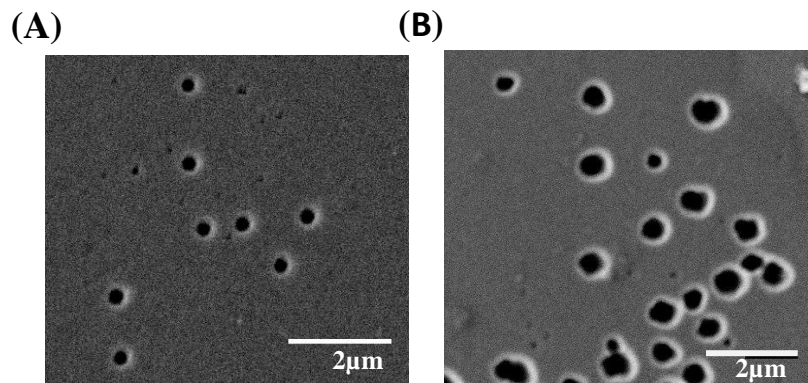


Figure 3.5: FESEM images of the binary mixtures in the (A) T1, and (B) T2 regions of the phase profile.

The QD-PDADMAC binary mixture shows turbidity profile in the range 22.4-160 µM. We have focused mainly on the T1 (25.6 µM) and T2 (130.0 µM) regions of the binary mixture. The turbidity is more in

the T2 region as compared to those in the T1 region. FESEM image in the T1 region [Figure 3.5. (A)], shows distinct spherical droplets with mean size of 383.9 ± 17.9 nm, while the droplets in the T2 region are much larger with mean size of 590.8 ± 23.8 nm [Figure 3.5. (B)]. Hence, the higher turbidity is due to the formation of larger self-assembled aggregates in the T2 region compared to the droplets in T1 region.

3.5. The effect of pH variation and ionic strength on the colloidal droplets formed in T1 and T2 region.

The interaction between two molecules and the nature of the complex formed between them is affected by different factors such as pH, ionic strength, concentration etc. Figure 3.6, shows the absorption spectra of variation of pH and ionic strength in T1 and T2 region.

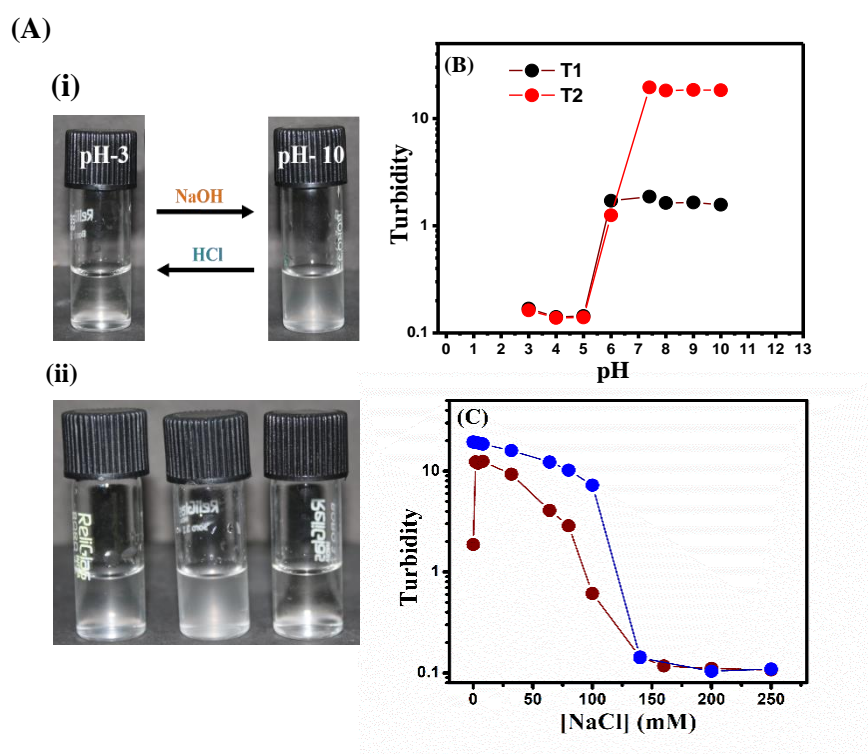


Figure 3.6: (A) (i) Photographs of QD-PDADMAC binary mixture at pH-3 and pH-10 (ii) Salt solution at different concentration ionic (B) variation in the turbidity of the binary mixture with respect to pH in the

solution to prepare the final concentrations of 2.0 μM (FITC), 20.0 μM (Rh6G), 1.0 μM (Nile blue), 59 μM (HSA), and 47.0 μM (BSA). These mixtures were kept for equilibrated for atleast 12h. Afterwards, these mixtures were again centrifuged at 10000 rpm for 30 min to separate the supernatant from the coacervate residue. The concentrations of dyes and proteins in the supernatant were determined using UV-vis spectroscopy. The partition coefficient (K) was calculated by the taking the ratio of the concentrations of dyes/proteins loaded in coacervates to the concentrations of dyes/proteins present in the supernatant

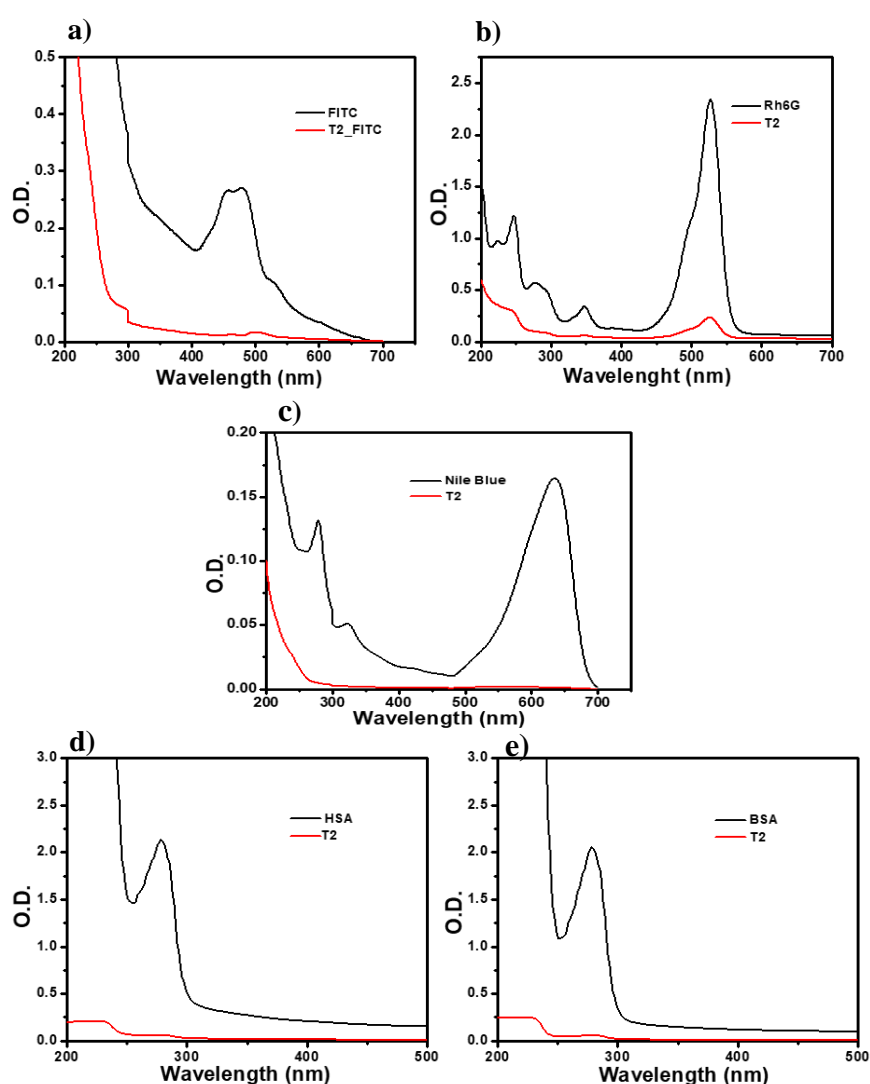


Figure 3.7: Absorption spectra of a) FITC, b) Rhodamine 6G, c) Nile blue, d) HSA and e) BSA with T2 (130 μM). The black represents the dyes and protein in aqueous solution.

Absorption spectra of both free and encapsulated dyes and proteins were taken. Generally, the absorption of the encapsulated molecule is same (if loading is 100%) or less than its free form. In this case, the absorbance of encapsulated dyes and proteins is less than its free form. The observed peaks in the beginning disappears after addition of aqueous solutions of the different dyes and proteins to the QD-PDADMAC binary mixture. This result suggest that the dyes and proteins are incorporated efficiently into the coacervate droplets via electrostatic interaction between these dyes/protein and the polymer without any structural disruption.

Table 1. Estimated partition coefficients (K) of dyes and proteins inside coacervate droplets (T2 region).

Systems	Concentration used	K
FITC	2 μ M	10.6 \pm 2.5
Rh6g	20 μ M	9.0 \pm 1.6
Nile blue	1 μ M	136.0 \pm 25.0
HSA	59 μ M	34.1 \pm 6.5
BSA	47 μ M	35.0 \pm 7.0

Chapter 4

Conclusion

In conclusion, using different types of spectroscopic techniques, we present the formation of self-assembled nanocomposites. These self-assembled nanocomposites are activated by the association of negatively charged CdTe QDs with positively charged PDADMAC to form spherical coacervate droplets in aqueous medium. The nanocomposites that are formed are stable in a wide range of composition, pH and ionic strength. Also, we present here a method for encapsulating dyes, such as FITC, Rhodamine 6G, Nile blue and proteins like HSA and BSA via the electrostatic interaction of the charged species. The unique luminescence properties observed for these droplets may have profound implications in various applications such as bioimaging, sensing, and light-emitting devices.

REFERENCES

- 1 <http://www.theguardian.com/nanotechnology-world/nanotechnology-in-everyday-life>
- 2 Bosnian A. W., Heumann A., and Klaerner G., (2001), *Am. Chem. Soc.* 123, 6461-6462
- 3 Tully D. C., Wilder K., and Frechet J. M. J., (1999), *Adv. Mater* 11, 314-318.
- 4 Townsen P., and Olivares J., (1997), *Appl. Surf. Sci.* 1 10, 275-282
- 5 Calander N., and Willander M., (2002), *Phys. Rev. Lett.* 89, 143-603
- 6 Boal A. K., Ilhan F., and DeRouchey J. E., (2000), *Nature* 404, 746-748
- 7 Haw M. D., Poon W. C. K., and Pusey P. N., (1997), *Physical Review E* 56, 1918-1933.
- 8 Pellegrino T., Kudera S., and Liedl T., (2005) *Small*, 1, 48.
- 9 Pinaud F., Clarke S., and Sittner A., (2010), *Nat. Methods*, 7, 275.
- 10 Lowe A. R., Siegel J. J., and Kalab P., (2010), *Nature*, 467, 600.
- 11 Riegler J. and Nann T., (2004), *Anal. Bioanal. Chem.*, 379, 913.
- 12 Zhang C. Y., Yeh H. C., and Kuroki M. T., (2005), *Nat. Mater.*, 4, 826.
- 13 Yao H. Q., Zhang Y., and Xiao F., (2007), *Angew. Chem., Int. Ed.*, 46, 4346.
- 14 Zhao L. and Lin Z. Q., (2012), *Adv. Mater.*, 24, 4353.
- 15 Bawendi M. G., Wilson W. L., and Rothberg L., (1990), *Phys. Rev. Lett.* 65, 1623-1626.
- 16 Brus L., (1991), *Applied Physics a-Materials Science & Processing* 53, 465-474.

- 17 Brus L. E., Szajowski, P. F., and Wilson, W. L., (1995), *J. Am. Chem. Soc.* 117, 2915-2922.
- 18 Chen C. C., Herhold A. B., and Johnson C. S., (1997), *Science*, 276, 398-401.
- 19 Chestnoy N., Hull R., and Brus L. E., (1986), *J. Chem Phys.* 85, 2237-2242
- 20 Empedocles S. A., and Bawendi M. G., (1997), *Science*, 278, 2114-2117.
- 21 Empedocles S., and Bawendi M., (1999), *Acct. Chem. Res.*, 32, 389-396.
- 22 Nirmal M., Dabbousi B. O., and Bawendi M. G., (1996), *Nature* 383, 802-804.
- 23 Nirmal M., and Brus L., (1999), *Acct. Chem. Res.* 32, 407-414.
- 24 Shim M., Wang C. J., and Guyot-Sionnest P., (2001), *J. Phys. Chem.B* 105, 2369- 2373.
- 25 Shim M., and Guyot-Sionnest P., (2001), *Phys. Rev. B* 6424, art. no.-245-342.
- 26 Shim M., Wang C. J., Norris, D. J., and Guyot-Sionnest P., (2001), *MRS Bulletin* 26, 1005-1008.
- 27 Qiang Z., Chen Y-M., Xia Y., Liang W., Zhu Y., and Vogt BD., (2017), Ultra-long cycle life, low-cost room temperature sodium-sulfur batteries enabled by highly doped (N, S) nanoporous carbons. *Nano Energy.* 32,59-66.
- 28 Qiang Z., Liu X., and Zou F., and Vogt BD., (2017), Bimodal Porous Carbon-Silica Nanocomposites for Li-Ion Batteries. *J Phys Chem C.* 121, 16702-16709
- 29 Wang C., Duan Y., and Zacharia NS., Vogt BD., (2017), A family of mechanically adaptive supramolecular graphene oxide/poly (ethylenimine) hydrogels from aqueous assembly. *Soft Matter.* 13,1161-1170.
- 30 Zhang H., Wang C., Zhu G., and Zacharia NS., (2016), Self-Healing of- Bulk Polyelectrolyte Complex Material as a

- Function of pH and Salt. *ACS Appl Mater Interfaces*. 8:26258-26265.
- 31 Wang C., Wiener CG., Cheng Z., Vogt BD, Weiss RA., (2016), Modulation of the mechanical properties of hydrophobically modified supramolecular hydrogels by surfactant-driven structural rearrangement. *Macromolecules*. 49, 9228-9238.
 - 32 Larson D.R., et al., (2003), Water-Soluble Quantum Dots for Multiphoton Fluorescence Imaging in Vivo. *Science*, 300, 1434-1436.
 - 33 John Wilson; et al, (2002). Synthesis and Use of PolyDADMAC for Water Purification.
 - 34 Research — Complex Coacervates, Tirrell Research Group.
 - 35 Vaishnav J. K., Mukherjee T. K., (2018), Long-Range Resonance Coupling-Induced Surface Energy Transfer from CdTe Quantum Dot to Plasmonic Nanoparticle. *J. Phys. Chem. Chem. Phys.* 122, 28324– 28336.
 - 36 Yu W., W., Qu L., Guo W., Peng X., (2003), Experimental Determination of the Extinction Coefficient of CdTe, CdSe, and CdS Nanocrystals. *Chem. Mater.* 15, 2854-2860.